Cannabidiol exerts sebostatic and antiinflammatory effects on human sebocytes

Attila Oláh,[1] Balázs I. Tóth,[1,2] István Borbíró,[1] Koji Sugawara,[3,4] Attila G. Szöllősi,[1] Gabriella Czifra,[1] Balázs Pál,[5] Lídia Ambrus,[1] Jennifer Kloepper,[4] Emanuela Camera,[6] Matteo Ludovici,[6] Mauro Picardo,[6] Thomas Voets,[2] Christos C. Zouboulis,[7] Ralf Paus,[4,8] and Tamás Bíró[1]

[1]DE-MTA "Lendület" Cellular Physiology Research Group, Department of Physiology, University of Debrecen, Debrecen, Hungary. [2]Laboratory for Ion Channel Research and TRP Research Platform Leuven, Department of Cellular and Molecular Medicine, KU Leuven, Leuven, Belgium. [3]Department of Dermatology, Osaka City University Graduate School of Medicine, Osaka, Japan. [4]Department of Dermatology, University of Lübeck, Lübeck, Germany. [5]Neurobiology Research Group, Department of Physiology, University of Debrecen, Debrecen, Hungary. [6]Laboratory of Cutaneous Physiopathology and Integrated Center of Metabolomics Research, San Gallicano Dermatologic Institute, IRCCS, Rome, Italy. [7]Departments of Dermatology, Venereology, and Allergology and Immunology, Dessau Medical Center, Dessau, Germany. [8]School of Translational Medicine, University of Manchester, Manchester, United Kingdom.

The endocannabinoid system (ECS) regulates multiple physiological processes, including cutaneous cell growth and differentiation. Here, we explored the effects of the major nonpsychotropic phytocannabinoid of *Cannabis sativa*, (-)-cannabidiol (CBD), on human sebaceous gland function and determined that CBD behaves as a highly effective sebostatic agent. Administration of CBD to cultured human sebocytes and human skin organ culture inhibited the lipogenic actions of various compounds, including arachidonic acid and a combination of linoleic acid and testosterone, and suppressed sebocyte proliferation via the activation of transient receptor potential vanilloid-4 (TRPV4) ion channels. Activation of TRPV4 interfered with the prolipogenic ERK1/2 MAPK pathway and resulted in the downregulation of nuclear receptor interacting protein-1 (NRIP1), which influences glucose and lipid metabolism, thereby inhibiting sebocyte lipogenesis. CBD also exerted complex antiinflammatory actions that were coupled to A2a adenosine receptor-dependent upregulation of tribbles homolog 3 (TRIB3) and inhibition of the NF-κB signaling. Collectively, our findings suggest that, due to the combined lipostatic, antiproliferative, and antiinflammatory effects, CBD has potential as a promising therapeutic agent for the treatment of acne vulgaris.

Introduction

Acne vulgaris is the most common human skin disease, affecting quality of life of millions worldwide. In spite of heroic basic and applied research efforts, we still lack indisputably curative anti-acne agents, which target multiple pathogenetic steps of acne (sebum overproduction, unwanted sebocyte proliferation, inflammation) and, moreover, which possess favorable side effect profiles (1, 2). Investigations over the last two decades have confirmed unambiguously that the human body expresses such receptors, which are able to specifically bind and recognize characteristic terpene-phenol compounds of the infamous plant *Cannabis sativa*, collectively referred to as phytocannabinoids. These receptors, their endogenous ligands (the endocannabinoids [eCBs]), and the enzymes involved in the synthesis and degradation of the eCBs collectively constitute the eCB system (ECS), a complex intercellular signaling network markedly involved in the regulation of various physiological processes (3–6).

Investigation of the cutaneous cannabinoid system seems to be a promising choice when searching for novel therapeutic possibilities (7, 8). Indeed, we have shown previously that the skin ECS regulates cutaneous cell growth and differentiation (9, 10), and it reportedly exerts antiinflammatory effects (11). Of further importance, we have also demonstrated that the ECS plays a key role in the regulation of sebum production (12). According to our recent findings, prototypic eCBs, such as N-arachidonoyl ethanolamide (anandamide [AEA]) and 2-arachidonoylglycerol, are constitutively produced in human sebaceous glands. Moreover, using human immortalized SZ95 sebocytes, we have also demonstrated that these locally produced eCBs (acting through a CB2 cannabinoid receptor→ERK1/2 MAPK→PPAR pathway) induce terminal differentiation of these cells, which is characterized by increased neutral lipid (sebum) production of the sebocytes (12). These findings confirmed unambiguously that human sebocytes have a functionally active ECS; yet, we did not possess data on the potential effect(s) of plant-derived cannabinoids.

(-)-Cannabidiol (CBD) is the most studied nonpsychotropic phytocannabinoid (13–15). It has already been applied in clinical practice without any significant side effects (Sativex) (16), and numerous ongoing phase II and III trials intend to explore its further therapeutic potential (17). Hence, within the confines of the current study, we intended to reveal the biological actions of CBD on the human sebaceous gland. Since we lack adequate animal models (18), we used human immortalized SZ95 sebocytes, the best available cellular system (19), and the full-thickness human skin organ culture (hSOC) technique (20).

Results

CBD normalizes "pro-acne agent"–induced excessive lipid synthesis of human sebocytes. We first assessed the biological effects of CBD

Conflict of interest: The authors have declared that no conflict of interest exists.
Submitted: March 17, 2014; **Accepted:** June 5, 2014.
Reference information: *J Clin Invest*. 2014;124(9):3713–3724. doi:10.1172/JCI64628.

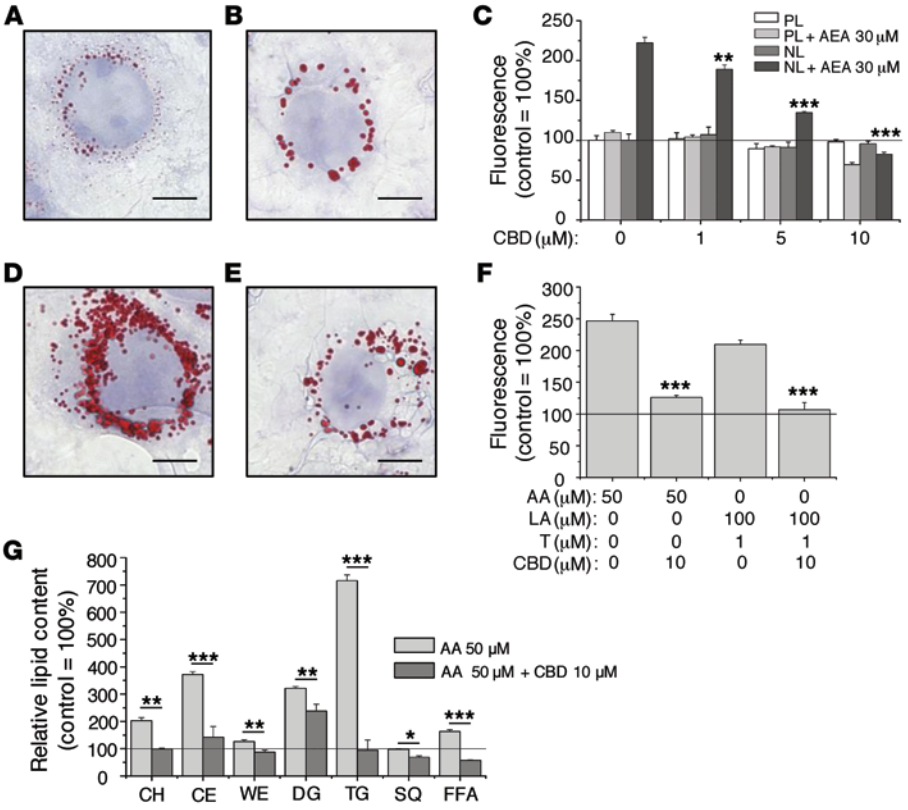

Figure 1. CBD prevents excessive lipogenesis induced by "pro-acne agents" in human SZ95 sebocytes. (**A**, **B**, **D**, and **E**) Semiquantitative determination of lipid synthesis for (**A**) control, (**B**) 10 μM CBD, (**D**) 30 μM AEA, and (**E**) 30 μM AEA plus 10 μM CBD (sebum droplets: Oil Red O staining, red; nuclei: hematoxylin, blue). Scale bars: 10 μm. (**C**) Quantitative determination of lipid synthesis (Nile Red staining). $^{**}P < 0.01$, $^{***}P < 0.001$ compared with the AEA-treated group. PL, polar lipids; NL, neutral lipids. (**F**) Neutral lipid synthesis (Nile Red staining). $^{***}P < 0.001$ compared with the respective AA- or LA-T–treated group. (**C** and **F**) Data are expressed as the percentage of the vehicle control (mean ± SEM of 4 independent determinations). The solid line indicates 100%. Two additional experiments yielded similar results. (**G**) Analysis of the sebaceous lipidome. Sebaceous lipid classes were analyzed by HPLC-ToF/MS in sebocytes. CH, free cholesterol; CE, cholesteryl esters; WE, wax esters; DG, diacylglycerols; TG, triacylglycerols; SQ, squalene; FFA, free fatty acids. Results are expressed as the percentage of the vehicle control (mean ± SD of 3 independent determinations). The solid line indicates 100%. Two additional experiments yielded similar results. $^{*}P < 0.05$, $^{**}P < 0.01$, $^{***}P < 0.001$.

(1–10 μM) on the lipogenesis of SZ95 sebocytes. Although eCBs are known to show intense lipogenic actions via the metabotropic CB2 receptors (12), neither semiquantitative Oil Red O nor quantitative Nile Red staining indicated changes in the basal neutral (sebaceous) lipid synthesis of SZ95 sebocytes following 24-hour CBD treatment (Figure 1, A–C) (or 48-hour CBD treatment; data not shown). Intriguingly, however, CBD markedly inhibited the lipogenic action of the prototypic eCB, AEA, in a dose-dependent manner (1–10 μM; Figure 1, C–E).

We also tested its effect on actions of other lipogenic substances, which were shown previously to act through different, ECS-independent signal transduction mechanisms. Indeed, CBD effectively inhibited lipid synthesis induced by either arachidonic acid (AA) (21) or the combination of linoleic acid and testosterone (LA-T) (ref. 22 and Figure 1F), indicating that the effect of CBD is not "ECS specific" but a "universal" lipostatic action.

Since cannabinoids have been very often shown to exert "biphasic" effects (i.e., opposing physiological actions at nM vs. μM concentrations) (23), we also tested the effects of lower (1–100 nM) CBD concentrations; notably, they did not influence either basal or AA-induced lipid synthesis of the sebocytes (Supplemental Figure 1; supplemental material available online with this article; doi:10.1172/JCI64628DS1).

We also investigated the effects of CBD on the lipidome of SZ95 sebocytes under in vitro conditions that mimicked "acne-like" circumstances (the latter was achieved by using a key "pro-acne" inflammatory mediator, AA) (1, 2, 21, 24–26). Importantly, CBD almost completely normalized the AA-enhanced "pathological" lipogenesis of SZ95 sebocytes (Figure 1G). This suggests that CBD may primarily normalize both quantitatively and qualitatively excessive and abnormal lipid production induced by acne-promoting stimuli.

CBD decreases proliferation, but not the viability, of human sebocytes both in vitro and ex vivo. Besides the above lipostatic action, another desired effect of a proper anti-acne agent would be to inhibit the unwanted growth of sebocytes (2, 27, 28). Of great importance, proliferation of SZ95 sebocytes was significantly reduced in the presence of CBD (1–10 μM) (Figure 2A). It should be noted, however, that CBD did not suppress the cell count below the "starting" number (measured at day 1), arguing for a "pure" antiproliferative effect. Indeed, the lack of its effects on the count of viable cells was further verified by showing that these concentrations of CBD did not decrease cellular viability or induce either apoptosis or necrosis of SZ95 sebocytes (Figure 2, B and C). Notably, administration of 50 μM CBD evoked apoptosis-driven cytotoxicity and, hence, led to decreased lipogenesis (Supplemental Figure 2, A–C). Likewise, elongated application of 10 μM CBD (6-day treatments) also decreased cell number and lipogenesis (Supplemental Figure 2, D and E).

Clinically, the key question is whether the above in vitro observations could be translated into significant sebostatic (i.e., lipostatic and antiproliferative) effects of CBD on human sebaceous glands in situ. To explore this on the preclinical level, the full-thickness hSOC technique (20) was used. These hSOC assays, which mimic the human sebaceous gland function in vivo as closely as this is currently possible on the ex vivo level, clearly demonstrated that application of CBD completely prevented the lipogenic action of AEA in situ and, in line with our long-term in vitro observations (Supplemental Figure 2E), decreased basal lipogenesis as well (Figure 2, D–H). Likewise, CBD markedly sup-

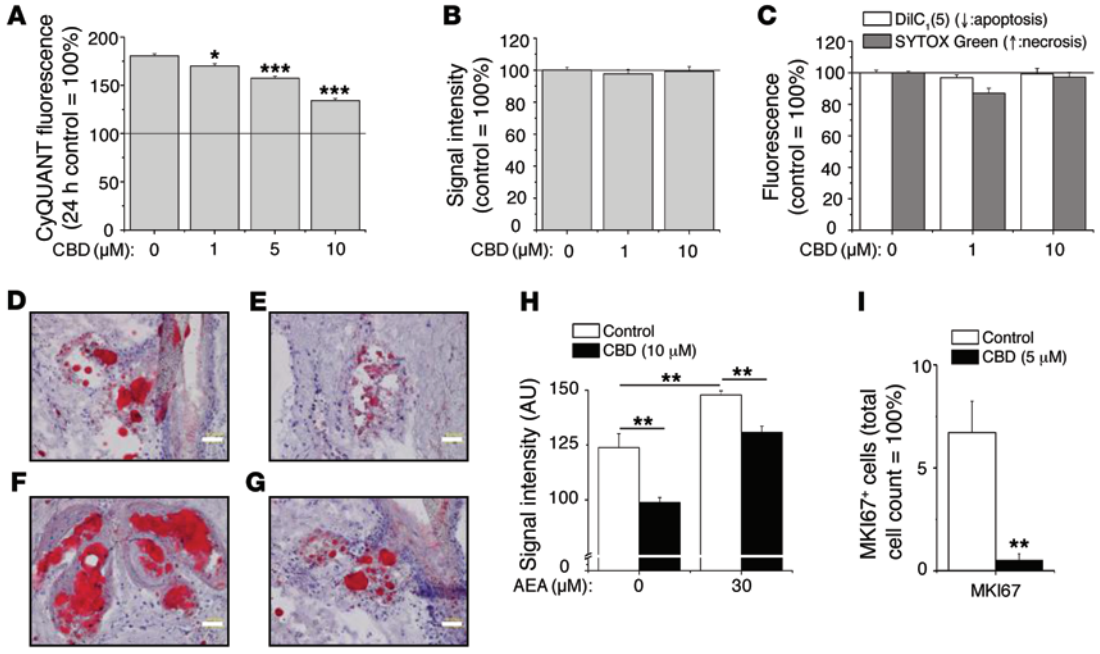

Figure 2. CBD exerts sebostatic effects in vitro and under "in vivo–like" circumstances. (**A**) CyQUANT proliferation assay after 72-hour treatments. $*P < 0.05$, $***P < 0.001$ compared with the 72-hour vehicle control. The solid line indicates the level of the 24-hour vehicle control. (**B**) MTT assay. Viability of sebocytes following 48-hour treatments. (**C**) Cell death [$DilC_1(5)$ and SYTOX Green double labeling] assays after 24-hour treatments. (**A**–**C**) Results are expressed as the percentage of the vehicle control (mean ± SEM of 4 independent determinations). The solid line indicates 100%.Two additional experiments yielded similar results. (**D**–**G**) hSOC of (**D**) control, (**E**) 10 μM CBD, (**F**) 30 μM AEA, and (**G**) 30 μM AEA plus CBD 10 μM (14 days; sebum: Oil Red O staining, red; nuclei: hematoxylin, blue). Scale bars: 50 μm. (**H**) Statistical analysis of the lipid production on 4 histological sections per group. Results are expressed as mean ± SEM. $**P < 0.01$. (**I**) Statistical analysis of the number of $MKI67^+$ cells as compared with the number of $DAPI^+$ cells on 2 histological sections per group (hSOC; 48 hours). $**P < 0.01$ compared with the vehicle control. Results are expressed as mean ± SEM.

pressed the expression of the proliferation marker MKI67 (Figure 2I). This suggests that CBD may also operate as a potent sebostatic agent in vivo when tested in appropriate clinical trials.

CBD exerts universal antiinflammatory actions. We additionally found that CBD also prevented the "pro-acne" LA-T combination from elevating the expression of *TNFA* (Figure 3A), a key cytokine in the pathogenesis of acne vulgaris (2, 24–30). These data suggested that CBD may exert antiinflammatory actions on human sebocytes (as had already been demonstrated for CBD in several other experimental models, such as diabetes, rheumatoid arthritis, etc.) (31). Therefore, in order to confirm the putative universal antiinflammatory action of the CBD on human sebocytes, we next assessed its effects by modeling both Gram-negative infections (applying the TLR4 activator LPS) and Gram-positive infections (using the TLR2 activator lipoteichoic acid [LTA]). We found that CBD completely prevented the above treatments from elevating *TNFA* expression (Figure 3). Moreover, CBD also normalized LPS-induced *IL1B* and *IL6* expression (Figure 3B) (expression of these 2 cytokines was found not to be modulated by 24-hour LA-T or LTA treatment; data not shown). Taken together, these results strongly suggest that CBD's universal sebostatic action is accompanied by substantial antiinflammatory effects, which would be very much desired in the clinical treatment of acne vulgaris (1, 2, 24–30).

Sebostatic (i.e., lipostatic and antiproliferative), but not antiinflammatory, actions of CBD are mediated by the activation of transient receptor potential vanilloid-4 ion channels. Next, we dissected the molecular mechanism(s) that underlie the remarkable lipostatic effects of CBD. As expected, neither CB1- nor CB2-specific antagonists (AM251 and AM630) were able to antagonize the lipid synthesis-inhibitory action of CBD (Supplemental Figure 3); hence, alternative options had to be considered.

First, we studied the effects of CBD on the ionic currents of SZ95 sebocytes. Using whole-cell patch-clamp configurations, membrane currents were elicited by voltage ramp protocols (Figure 4, A and B) and then normalized to cell membrane capacitance at two different potentials, i.e., at –90 and +90 mV (Figure 4C). CBD (10 μM) induced a mostly outwardly rectifying current and a positive shift in the reversal potential, arguing for the activation of certain cation channels upon CBD application.

It is well known that various cannabinoids can modulate the activity of certain transient receptor potential (TRP) channels, collectively referred to as "ionotropic cannabinoid receptors" (32–37). Moreover, we have shown recently that activation of TRP vanilloid-1 (TRPV1) on SZ95 sebocytes by capsaicin also exerts potent lipostatic actions (38). Therefore, we first systematically explored these candidate "CBD targets."

We found that SZ95 sebocytes express TRPV1, TRPV2, and TRPV4 both at the mRNA and protein levels (Supplemental Figure 4, A–C). Among these TRP channels, *TRPV4* showed the highest mRNA levels by far (expression of *TRPA1* and *TRPM8* was below the detection limit; data not shown).

Since the 3 identified TRPs are nonselective cation channels that are most permeable to Ca^{2+} (39), we studied the effects of CBD on the calcium homeostasis of the sebocytes. Using a fluorescent

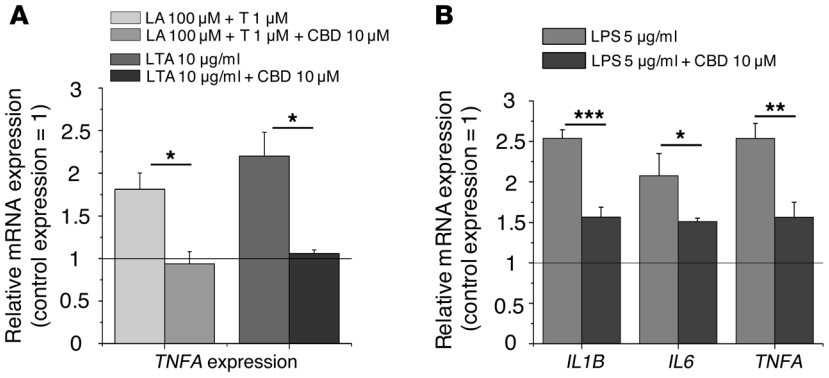

Figure 3. CBD exerts universal antiinflammatory actions. (**A**) *TNFA* mRNA expression following 24-hour "pro-acne" lipogenic and TLR agonist treatments with or without CBD. $^*P < 0.05$ compared with the corresponding CBD-free treatments. (**B**) *IL1B*, *IL6*, and *TNFA* mRNA expression following 24-hour LPS treatment with or without CBD. $^*P < 0.05$, $^{**}P < 0.01$, $^{***}P < 0.001$ compared with the corresponding CBD-free treatments. (**A** and **B**) Data are presented using the ΔΔCT method; *GAPDH*-normalized mRNA expression of the vehicle control was set as 1 (solid line). Data are expressed as mean ± SD of 3 independent determinations. Two additional experiments yielded similar results.

Ca^{2+}-imaging technique, we found that CBD significantly increased the intracellular calcium concentration ($[Ca^{2+}]_{IC}$) of SZ95 sebocytes (Figure 5, A and B). This action was equally antagonized by (a) the decrease of the extracellular Ca^{2+} concentration ($[Ca^{2+}]_{EC}$); (b) the nonspecific TRP channel blocker ruthenium red; and, of great importance, (c) the TRPV4-specific antagonist HC067047 (HC) (Figure 5, A and B). We have also shown that the suppression of $[Ca^{2+}]_{EC}$ or the coapplication of HC also prevented the lipostatic action of CBD (Figure 5C); notably, the TRPV4 antagonist alone did not affect basal lipid synthesis (Supplemental Figure 5).

To further confirm the functional expression of TRPV4 on human sebocytes, the TRPV4-specific ultrapotent agonist GSK1016790A (GSK) was applied. The agonist evoked membrane currents, which were prevented by the specific TRPV4 antagonist HC (Supplemental Figure 6, A and B), indicating that TRPV4 channels are indeed functionally expressed in human sebocytes. Moreover, GSK mimicked both the CBD-induced $[Ca^{2+}]_{IC}$ elevations (Supplemental Figure 6, C and D) and CBD's lipostatic actions (Figure 5C). Since the CBD-evoked lipostatic effects and the induced Ca^{2+} signals were not influenced by the TRPV1-specific antagonists, capsazepine (Supplemental Figure 7, A–C) or AMG 9810 (data not shown), these electrophysiological, Ca^{2+}-imaging and cellular physiology data collectively argued for the selective involvement of TRPV4 (but not of TRPV1) in mediating the effects of CBD.

To further validate this concept, knockdown of TRPV1, TRPV2, and TRPV4 by RNA interference (RNA_i) was used (quantitative "real-time" PCR [Q-PCR] and Western blot analyses verified the successful silencing of the targeted TRPVs; Supplemental Figure 8, A–F). We showed that neither TRPV1 nor TRPV2 silencing significantly influenced the lipostatic action of CBD (Supplemental Figure 9, A and B). In contrast, TRPV4-specific "knockdown" was able to prevent this effect of CBD (Figure 5D) as well as the increase of $[Ca^{2+}]_{IC}$ (Supplemental Figure 10) and the lipid-lowering action of the TRPV4-specific activator GSK (Figure 5E). Collectively, these data unambiguously confirm that CBD activates TRPV4 and that this ion channel selectively mediates its lipostatic action.

Interestingly, we also showed that, similar to the lipostatic action, antagonism of TRPV4 was able to significantly prevent the antiproliferative effect of CBD (Figure 6A). However, quite surprisingly, antiinflammatory actions of CBD were not affected by the antagonist (Figure 6B); these latter findings suggested that these antiinflammatory actions might be a TRPV4-independent process.

Sebostatic action of CBD is mediated by TRPV4-dependent interference with the ERK1/2 MAPK pathway and downregulation of nuclear receptor interacting protein-1. To dissect the intracellular signaling pathways that underlie the above effects, we first investigated the putative participation of several kinases (i.e., PKC isoforms, PI3K, PKA) as well as calcineurin in mediating the lipostatic effects of CBD. Notably, inhibition of activities of these molecules had no effect on the lipostatic activity of CBD (Supplemental Figure 11, A and B).

Then, in order to identify target genes and pathways regulated (directly or indirectly) by CBD, genome-wide microarray analyses were performed on 3 independent sets of control and CBD-treated SZ95 sebocytes (10 μM CBD for 24 hours). Gene set enrichment

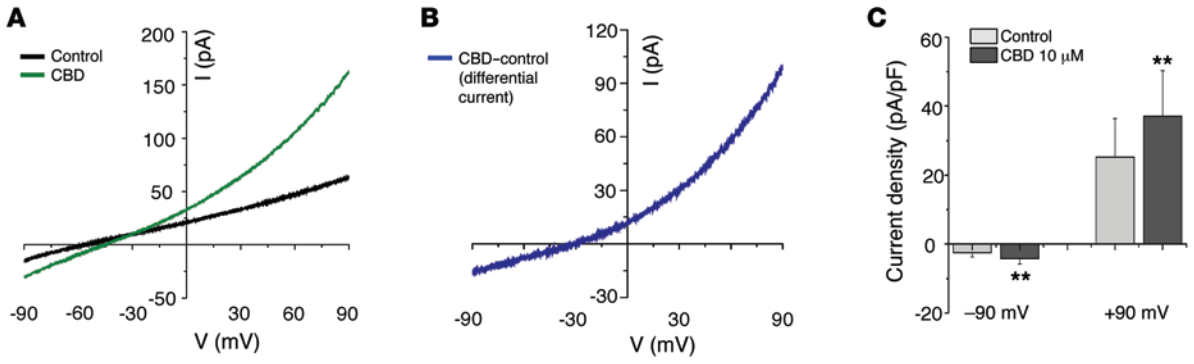

Figure 4. CBD induces outwardly rectifying membrane currents on human sebocytes. (**A**) Representative current-voltage traces of patch-clamp measurement of sebocytes using conventional whole-cell configuration with or without 10 μM CBD. (**B**) CBD-induced differential current (i.e., CBD minus control). (**C**) Averaged current densities measured at –90 mV and +90 mV of 7 cells. Results are expressed as mean ± SEM. $^{**}P < 0.01$ compared with control.

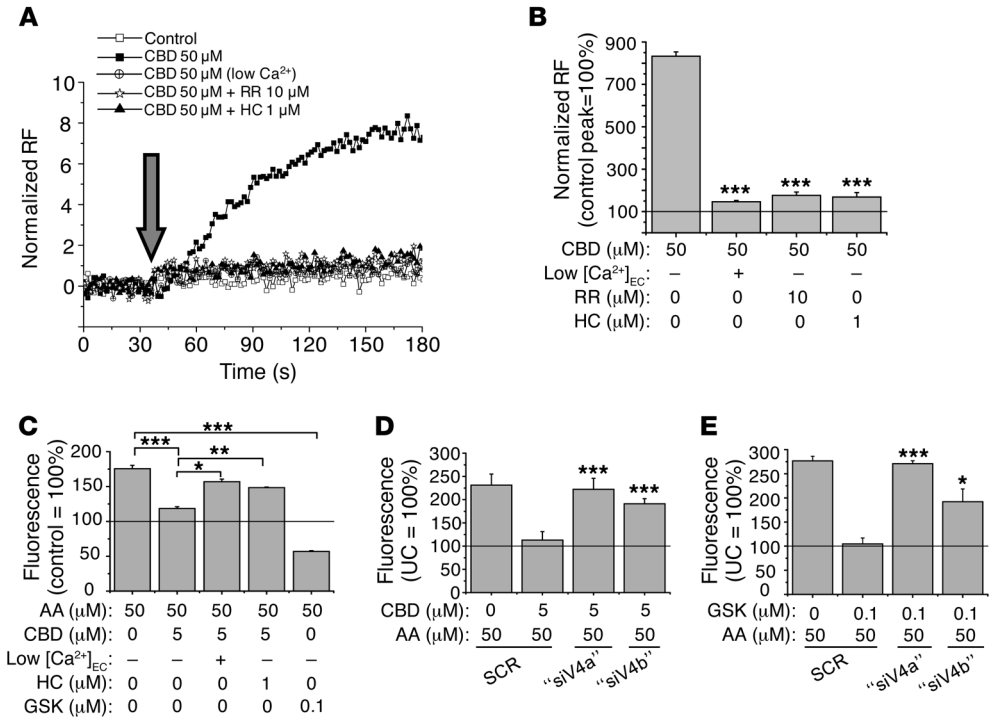

Figure 5. Lipostatic activity of CBD is mediated by TRPV4. (**A**) Fluorescent Ca^{2+} imaging. Compounds were applied as indicated by the arrow. Fluorescence (measured in relative fluorescence units [RF]) was normalized to the baseline. "Low $[Ca^{2+}]_{EC}$" indicates the use of nominally Ca^{2+}-free Hank's solution. Two additional experiments yielded similar results. (**B**) Statistical analysis of the fluorescent Ca^{2+}-imaging data. Fluorescence (expressed in RF) was normalized to the baseline. Measured peak values were expressed as the percentage of the baseline (mean ± SEM of 3 independent determinations). The solid line indicates 100%. Two additional experiments yielded similar results. ***$P < 0.001$ compared with the CBD-treated group. (**C**) Neutral lipid synthesis (Nile Red staining). Data are expressed as the percentage of the vehicle control (mean ± SEM of 4 independent determinations). The solid line indicates 100%. Two additional experiments yielded similar results. "Low $[Ca^{2+}]_{EC}$" indicates the use of low-Ca^{2+} Sebomed medium. *$P < 0.05$, **$P < 0.01$, ***$P < 0.001$. (**D** and **E**) Neutral lipid synthesis (Nile Red staining) following selective gene silencing of TRPV4 channel (24-hour treatments, started at day 3 after the transfection). Data are expressed as the percentage of the untransfected vehicle control (mean ± SEM of 4 independent determinations). The solid line indicates 100%. Two additional experiments yielded similar results. *$P < 0.05$, ***$P < 0.001$ compared with the SCR cells. "siV4a" and "siV4b" mark 2 different siRNA constructs against TRPV4. SCR, scrambled control; UC, untransfected vehicle control.

analysis (GSEA) (40–42) of the microarray results revealed that numerous mitosis and cell cycle (e.g., "mitosis," "G_2/M transition," "cell cycle," etc.), inflammation (e.g., "cytokine production," "cytokine biosynthetic process," "TLR9 pathway," "positive regulation of IκB kinase NF-κB cascade," etc.), and lipid synthesis–related ("acyltransferase activity," "lipid biosynthetic process," "positive regulation of MAPK activity," etc.) gene sets were identified among the downregulated ones, confirming our previous findings on the complex anti-acne effects of CBD. Moreover, downregulation of some "acne-related" gene sets (e.g., "IGF-1 pathway" and "mTOR pathway") (2, 43) also argued for the putative in vivo anti-acne efficiency of CBD. Further, upregulation of the "calcium signaling pathway" gene set confirmed the involvement of (TRPV4-dependent) calcium signaling (detailed results of GSEA are available in Supplemental Excel files 1 and 2).

During further data processing, Biological Networks Gene Ontology (BiNGO) analysis (44, 45) was also performed (see Supplemental Excel files 3 and 4; the hierarchy of the different gene ontology terms enriched among the downregulated and upregulated genes is summarized in Supplemental Figures 12 and 13, respectively). In line with our previous results, this method also highlighted that CBD exerted "anti-differentiating" effects on sebocytes (terms like "negative regulation of fat cell differentiation" and "negative regulation of fatty acid biosynthetic process" were found to be enriched among the upregulated genes).

Although these analyses further confirmed our previous findings on the complex anti-acne effects of CBD, we still aimed to recognize target genes that might be involved in mediating the different anti-acne modalities and/or might further strengthen the putative in vivo efficiency of CBD. Therefore, using rigid exclusion criteria (at least 2-fold changes in the corresponding expression levels equidirectional changes in all cases, and global, corrected $P < 0.05$), we found that 80 genes were significantly downregulated, whereas 72 genes were significantly upregulated by CBD treatment (microarray results are accessible through GEO series accession number GSE57571; downregulated and upregulated genes, together with their averaged fold changes, are summarized in Supplemental Tables 1 and 2). By using Q-PCR, we have confirmed that, following CBD treatment, expression of Rho GTPase-activating protein 9 (ARHGAP9, an endogenous inhibitor of the prolipogenic ERK signaling) (46) was upregulated, whereas the proliferation marker *MKI67* was downregulated (Figure 6C). (This latter result perfectly confirmed our findings obtained in hSOC experiments [Figure 2I].) Moreover, also in line with our previous findings, we found that TRPV4 antagonism could successfully prevent both alterations (Figure 6C).

It is well known that activation of the ERK1/2 MAPK pathway plays a crucial role in the regulation of cellular proliferation (47). Furthermore, we have demonstrated recently that this pathway is involved in mediating the "prolipogenic" action of AEA on human sebocytes (12). Considering that administration of CBD led to opposing cellular effects (i.e., decreased lipogenesis and proliferation) and upregulation the ERK inhibitor *ARHGAP9*, we hypothesized that CBD might inhibit MAPK activation. Indeed, AEA treatment was able to activate the ERK1/2 MAPK cascade (as monitored by assessing the level of phosphorylated ERK1/2 [P-ERK1/2]), an effect that was completely abrogated by the coadministration of

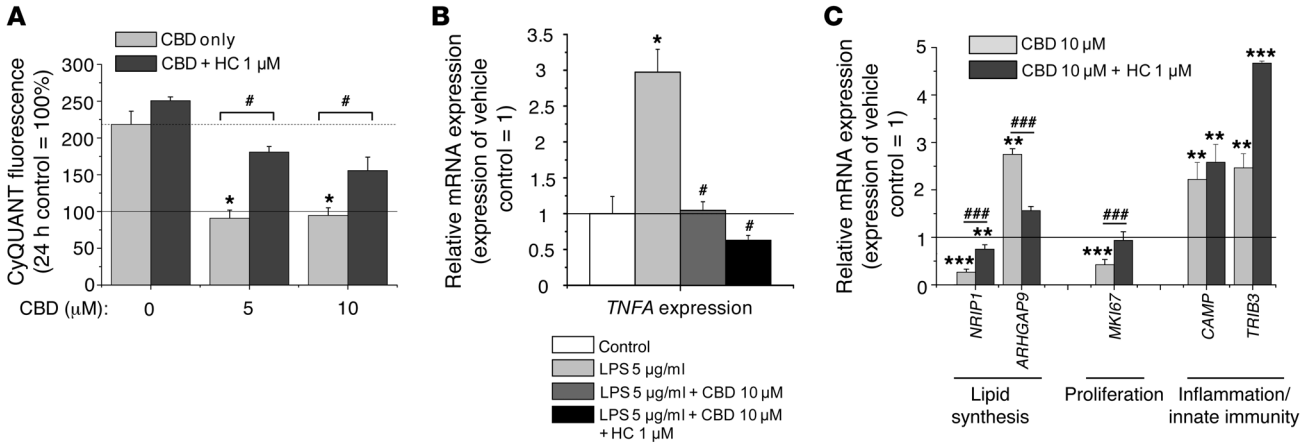

Figure 6. Anti-acne actions of CBD are mediated by parallel, partly independent signaling mechanisms. (**A**) CyQUANT proliferation assay after 72-hour treatments. $^{*}P < 0.05$ compared with the vehicle control. $^{\#}P < 0.05$. The solid line indicates the level of the 24-hour vehicle control. Dashed line indicates the level of the 72-hour vehicle control. Results are expressed as the percentage of the 24-hour vehicle control (mean ± SEM of 4 independent determinations). (**B**) *TNFA* mRNA expression following 24-hour LPS treatments with or without CBD and HC. $^{*}P < 0.05$ compared with the vehicle control; $^{\#}P < 0.05$ compared with the CBD-free LPS-treated group. Data are presented using the ΔΔCT method; peptidyl-prolyl isomerase A–normalized (*PPIA*-normalized) *TNFA* mRNA expression of the vehicle control was set as 1. Data are expressed as mean ± SD of 3 independent determinations. Two additional experiments yielded similar results. (**C**) Validation of the key microarray results. mRNA expression of various target genes following 24-hour CBD treatments with or without HC. $^{**}P < 0.01$, $^{***}P < 0.001$ compared with the vehicle control. $^{\#\#\#}P < 0.001$. Data are presented using the ΔΔCT method; *PPIA*-normalized mRNA expression of the vehicle control was set as 1 (solid line). Data are expressed as mean ± SD of 3 to 6 independent determinations. Two additional experiments yielded similar results.

CBD (Figure 7A). In a perfect agreement with our previous data (Figure 5, C–E, and Figure 6, A and C), this interference was found to be TRPV4 dependent, since the specific antagonist HC was able to fully prevent the effect of CBD (Figure 7A). This, again, confirmed the crucial role of TRPV4 activation in initiating the lipostatic and antiproliferative signaling cascade(s) of CBD.

We have also demonstrated that expression of nuclear receptor interacting protein-1 (*NRIP1*, also known as *RIP140*; a corepressor essential for triglyceride storage in adipose tissue) (48) was downregulated in a TRPV4-dependent manner (Figure 6C). We have shown that silencing of NRIP1 (validated by Q-PCR and Western blotting; Supplemental Figure 14, A and B) mimicked the lipostatic effect of CBD (Figure 7B), suggesting that downregulation of NRIP1 is indeed an important final effector of the lipid synthesis-inhibitory activity of CBD.

Antiinflammatory action of CBD is mediated by upregulation of tribbles homolog 3 and inhibition of the NF-κB pathway. Our microarray data have also highlighted the putative involvement of several innate immunity/inflammation-related genes in mediating the antiinflammatory action of CBD (Supplemental Tables 1 and 2). By using Q-PCR, we confirmed that expression of LL-37 cathelicidin (a key antimicrobial peptide expressed by and shown to be active in human sebocytes) (49) and tribbles homolog 3 (*TRIB3*, also known as *SINK*; a negative regulator of proinflammatory NF-κB signaling) (50) was upregulated by CBD. Importantly (again, in line with our previous results [Figure 6B]), these CBD-induced gene expression changes were not prevented by the coadministration of the TRPV4 antagonist HC (Figure 6C). When assessing the functional role of TRIB3, we found that, after its selective silencing (Supplemental Figure 15, A and B), CBD was unable to exert its antiinflammatory action to prevent LPS-induced *IL1B* and *IL6* upregulation (Figure 8A); in contrast, its lipostatic activity was not altered (Supplemental Figure 15C).

TRIB3 is known to inhibit the NF-κB pathway (50), and, furthermore, CBD has already been reported to exert its antiinflammatory actions via inhibition of the NF-κB signaling (51). Importantly, we found that CBD cotreatment indeed prevented the LPS-induced phosphorylation (hence inactivation) of the inhibitory IκBα and phosphorylation (hence activation) of the p65

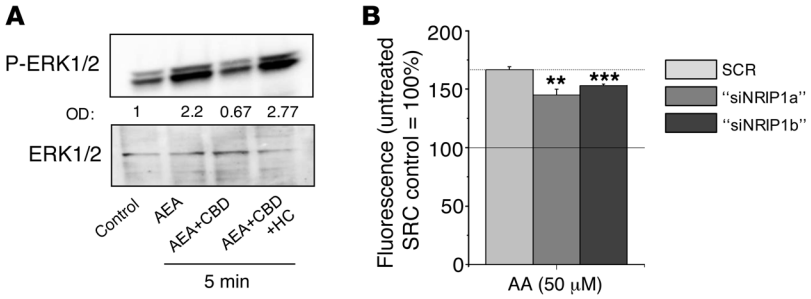

Figure 7. Lipostatic effects of CBD are mediated by TRPV4-dependent inhibition of the prolipogenic ERK1/2 signaling and downregulation of NRIP1. (**A**) Western blot analysis of lysates of SZ95 sebocytes treated with 30 μM AEA, 10 μM CBD, and 1 μM HC for 5 minutes. Numbers on the OD row indicate the optical density of the P-ERK1/2 bands normalized to the corresponding ERK1/2 signals. (**B**) Quantitative determination of neutral lipid synthesis (Nile Red staining; 24-hour treatments started at day 3 after transfection). $^{**}P < 0.01$, $^{***}P < 0.001$ compared with the scrambled (SCR) control group. "siNRIP1a" and "siNRIP1b" mark 2 different siRNA constructs against NRIP1. Data are expressed as the percentage of the SCR vehicle control (mean ± SEM of 4 independent determinations). The solid line indicates 100%.One additional experiment yielded similar results.

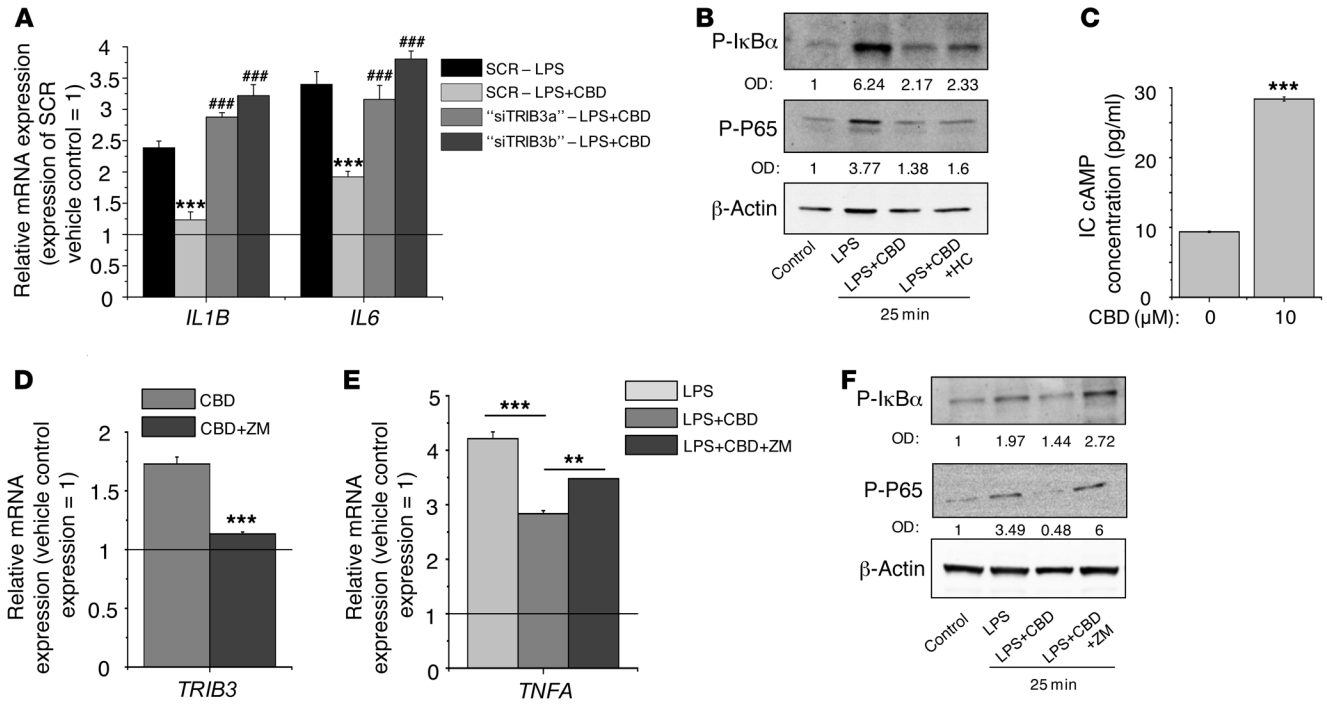

Figure 8. Antiinflammatory actions of CBD are coupled to A2a receptor-dependent upregulation of TRIB3 and subsequent inhibition of the P65-NF-κB signaling. (**A**) *IL1B* and *IL6* mRNA expression following 5 μg/ml LPS treatment with or without 10 μM CBD (24-hour treatments started at the day 2 after the transfection). ***$P < 0.001$ compared with the corresponding CBD-free treatments. ###$P < 0.001$ compared with the SCR group receiving the same treatments. "siTRIB3a" and "siTRIB3b" mark 2 different siRNA constructs against TRIB3. (**B**) Western blot analysis of lysates of SZ95 sebocytes treated with 5 μg/ml LPS, 10 μM CBD, and 1 μM HC for 25 minutes. (**C**) Determination of the intracellular cAMP concentration following 1-hour CBD (10 μM) or vehicle treatment. Data are presented as mean ± SEM of 3 independent determinations. One additional experiment yielded similar results. (**D** and **E**) *TRIB3* and *TNFA* mRNA expression following the indicated treatments (5 μg/ml LPS, 10 μM CBD, and 10 nM ZM). (**A**, **D**, and **E**) Data are presented using the ΔΔCT method; *PPIA*-normalized mRNA expression of the vehicle control was set as 1 (solid line). Data are expressed as mean ± SD of 3 independent determinations. One additional experiment yielded similar results. (**C**–**E**) **$P < 0.01$, ***$P < 0.001$. (**F**) Western blot analysis of lysates of SZ95 sebocytes treated with 5 μg/ml LPS, 10 μM CBD, and 100 nM ZM for 25 minutes. (**B** and **F**) Numbers on the OD row indicate the optical density of the P-IκBα and P-P65 bands normalized to the corresponding β-actin signals.

(RelA) NF-κB isoform (Figure 8B). These data indicate that, irrespective of the investigated cell type, interference with the NF-κB pathway could be an important mechanism in the development of the antiinflammatory actions of CBD. It should also be noted that TRPV4 antagonism exerted only negligible effects on the action of CBD (Figure 8B), again confirming that antiinflammatory activity of CBD is a TRPV4-independent process.

CBD induces a novel (A2a adenosine receptor→cAMP→TRIB3⊣NF-κB) antiinflammatory pathway. Finally, we aimed at identifying the target molecule of CBD, which, via the upregulation of TRIB3, mediates the antiinflammatory action of the phytocannabinoid. Since previous data suggested that elevation of the intracellular cAMP level is one of the possible inducers of TRIB3 activation/upregulation (52), we have investigated the effects of CBD on the cAMP level. CBD treatment indeed elevated the intracellular cAMP concentration of the sebocytes (Figure 8C), arguing that a G_s protein–coupled receptor might be the primary target of CBD. A previous finding that, in a murine model of acute lung injury, the G_s protein–coupled A2a adenosine receptor was found to mediate the antiinflammatory actions of CBD (53) made this receptor a very probable target in our system as well. Indeed, we found that the A2a receptor was expressed by human sebocytes both at the mRNA and protein levels (Supplemental Figure 16, A–C). In addition, we have also shown that application of a specific A2a receptor antagonist, ZM241385 (ZM), was able to significantly prevent the upregulation of TRIB3 by CBD (Figure 8D). Moreover, ZM also suppressed the antiinflammatory effect of the phytocannabinoid as well as the CBD-evoked inhibition of LPS-induced NF-κB activation (Figure 8, E and F). These intriguing findings collectively argued that activation of the "A2a receptor→cAMP→TRIB3⊣NF-κB" axis indeed plays a crucial role in mediating the antiinflammatory actions of CBD.

Discussion

In this study, we provide the first evidence that the nonpsychotropic phytocannabinoid CBD, which is already applied in clinical practice (16), exerted a unique "trinity of cellular anti-acne actions." Namely, CBD, without compromising viability (Figure 2, B and C), (a) normalized the pathologically elevated lipogenesis induced by "pro-acne" agents, both in a quantitative and qualitative manner (universal lipostatic effect; Figure 1); (b) suppressed cell proliferation (antiproliferative effect; Figure 2A); and (c) prevented the actions of TLR activation or "pro-acne" agents to elevate proinflammatory cytokine levels (universal antiinflammatory effect; Figure 3). Furthermore, we have shown that sebostatic actions of CBD also developed under "in vivo–like" conditions (hSOC; Figure 2, D–I).

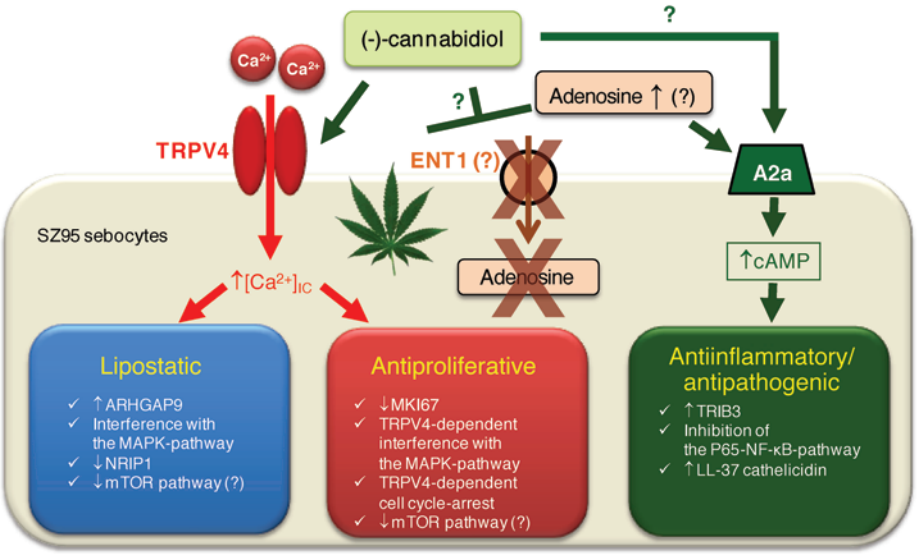

Figure 9. Schematic overview of the cellular "anti-acne trinity" of CBD and its proposed mechanism of action. For details, see Discussion section.

Besides the discussed "sebocyte-specific" steps of the pathogenesis of acne, promisingly targeted by the "cellular anti-acne trinity" of CBD, one should also keep in mind that there are additional factors, which contribute to the progression of the disease: the infundibular hyperproliferation/hyperkeratinization, leading to comedogenesis and subsequent overgrowth of "acnegenic" *Propionibacterium acnes* strains (2). It is very important to note that, based on the literature, administration of CBD holds out the promise to target these factors as well. Indeed, CBD was shown to inhibit proliferation of hyperproliferative keratinocytes (54), and it was demonstrated to possess remarkable antibacterial activity (55). Although its efficiency against "acnegenic" *Propionibacterium acnes* strains is not yet investigated, one can speculate that its putative indirect antibacterial activity (mediated by the upregulation of the expression of the antimicrobial peptide LL-37 cathelicidin [Supplemental Table 2 and Figure 6C]) could be further supported by direct bactericide effects, arguing that CBD might be very likely to behave as a potent anti-acne agent in vivo.

Given that sebum production is the result of holocrine secretion, the amount of sebum produced is at least as dependent on the proliferative activity of basal layer sebocytes in the sebaceous gland as on the amount of lipogenesis that individual sebocytes engage in (27, 28). Therefore, the novel and significant antiproliferative activity of CBD on human sebocytes in vitro and ex vivo documented here (Figure 2, A and I) is expected to greatly reduce sebum production in vivo. Moreover, it is also important to emphasize that, clinically, it is highly desirable that basal sebogenesis and viability of sebocytes are unaffected (Figure 1, A–C, and Figure 2, A–C) by CBD (at least in the noncytotoxic concentrations and after short-term treatments; Supplemental Figure 2, A–E), since a sufficient level of sebum production is a critical factor for maintaining proper function of the epidermal barrier, one of the central components of skin homeostasis (56).

CBD has already been shown to activate (e.g., certain TRP channels, α1 and 5-HT1a receptor, etc.), antagonize (e.g., TRPM8 and 5-HT3 receptor as well as "classical" [CB1 and CB2] and "novel" [GPR55] cannabinoid receptors, etc.), or allosterically modulate (e.g., μ- and δ-opioid receptors, etc.) the activity of a plethora of different receptors and, furthermore, to influence various other cellular targets (e.g., cyclooxygenase and lipoxygenase enzymes, fatty acid amide hydrolase, eCB membrane transporter, phospholipase A2, voltage-dependent anion channel 1, etc.) (15, 32–37, 57–60). Therefore, exploration of its exact mechanism of action appeared to be a great challenge. The fact that we have shown previously that activation of TRPV1 can evoke similar lipostatic effects (38) as those found for CBD (Figure 1 and Figure 2, D–H), together with our present findings that CBD induced membrane currents on sebocytes (Figure 4), prompted us to first investigate the role of TRP channels in mediating the above anti-acne modalities. We discovered that the lipostatic and antiproliferative effects of CBD were mediated by the activation of TRPV4 (and not TRPV1 or TRPV2) ion channels (Figures 5, C–E, and Figure 6A) and the concomitant increase in $[Ca^{2+}]_{IC}$. Actually, the "negative regulation" of lipogenesis by the elevation of $[Ca^{2+}]_{IC}$ is not unprecedented, since it has already been described in sebocytes (38) as well as in adipocytes (61, 62). It is also important to note that, within the confines of another study, we have shown that extracellular Ca^{2+} plays an important negative regulatory role in the sebaceous lipogenesis (C.C. Zouboulis et al., unpublished observations). Of further importance, we have also shown that the antiinflammatory activity of CBD is a TRPV4-independent process (Figure 6B).

Importantly, our data are in perfect agreement with the recent findings of De Petrocellis et al. (37). Using heterologous expression systems, they demonstrated that CBD is a potent but less efficacious activator of rat TRPV4 (as compared with the "classical" agonists or certain other phytocannabinoids, such as cannabichromene [CBC] or cannabidivarin [CBDV]). Although the possibility that CBD might be a more efficacious activator of human TRPV4 than of rat TRPV4 should also be taken into consideration; preliminary data of our recently started assessment of the putative anti-acne effects of other phytocannabinoids also suggest that CBC and CBDV possess an even more pronounced lipostatic efficiency than CBD, which further argues for the central role of TRPV4 (A. Oláh et al., unpublished observations).

In order to identify additional downstream targets, genome-wide microarray experiments were performed on 3 independent sets of control and CBD-treated (10 μM for 24 hours) sebocytes. GSEA (40–42) and BiNGO analysis (44, 45) of the microarray results uniformly confirmed our results, arguing for complex anti-acne actions upon CBD administration, as indicated by downregulation of inflammation (e.g., "cytokine production"), lipid synthesis (e.g., "lipid biosynthetic process" and "positive regulation of MAPK activity"), proliferation-related (e.g., "mitosis" and "G_2/M transition"), and "general pro-acne" (e.g., "mTOR pathway" and "IGF-1 pathway") (2, 43) gene sets and BiNGO terms (Supplemental Excel files 1–4 and Supplemental Figures 12 and 13).

Besides the above results, microarray analyses also revealed that levels of 80 genes were downregulated upon CBD treatment, whereas expression of 72 genes was upregulated upon CBD treatment, among which multiple potential "anti-acne" effectors were identified (Supplemental Tables 1 and 2). Q-PCR validation of the most promising target genes revealed that (in agreement with our cell physiology data) expression of lipid synthesis–related (*NRIP1* and *ARHGAP9*) and proliferation-related (MKI67) genes was altered in a TRPV4-dependent manner, whereas changes in the expression of "inflammation" genes were found to be TRPV4 independent (Figure 6C). Moreover, alterations of *ARHGAP9* expression (a known endogenous inhibitor of ERK signaling) (46) suggested that inhibition of the prolipogenic MAPK pathway (12) might play a role in mediating the lipostatic effects of CBD. Indeed, we found that CBD inhibited AEA-induced (prolipogenic) (12) ERK1/2 phosphorylation in a TRPV4-dependent manner (Figure 7A), confirming again the crucial role of TRPV4 in mediating the action of CBD.

We also silenced another "lipid-regulating gene" (i.e. *NRIP1*) (Supplemental Figure 14, A and B). As expected (48), knockdown of NRIP1 was able to mimic the lipostatic effect of CBD (Figure 7B).

Next, we aimed at revealing the signaling pathway of the anti-inflammatory actions. Thorough assessment of the microarray data highlighted the putative role of TRIB3, a known inhibitor of proinflammatory NF-κB signaling (50). In addition, inhibition of NF-κB signaling plays a crucial role in the development of CBD-mediated antiinflammatory actions in other systems (51). RNA_i-mediated selective gene silencing of TRIB3 in human sebocytes (Supplemental Figure 15, A and B) fully abrogated the ability of CBD to inhibit LPS-induced proinflammatory responses (Figure 8A). Although a previous study would have suggested it (63), interestingly, TRIB3 was found not to participate in mediating the lipostatic effects of CBD in sebocytes (Supplemental Figure 15C).

It is also noteworthy that TRIB3 has been identified recently as a potent phytocannabinoid target gene (64–66). These results, together with our data presented here, strongly argue for the key participation of TRIB3 in mediating cellular effects of cannabinoids.

Although CBD-dependent upregulation of its several known target genes, such as activating transcription factor 4, asparagine synthetase, cation transport regulator-like 1, and DNA-damage-inducible transcript 3 (refs. 66, 67, and Supplemental Tables 1 and 2), also argued for the activation of a TRIB3-dependent signaling pathway, to further strengthen the "TRIB3-hypothesis," we have also investigated the effects of CBD on one of the major cellular targets of TRIB3, i.e., NF-κB. As expected (51), CBD was able to inhibit LPS-induced NF-κB activation (again, in a TRPV4-independent manner; Figure 8B), which can fully explain its previously demonstrated antiinflammatory actions.

Finally, we aimed at identifying the upstream signaling of the TRIB3 activation/upregulation by CBD. We found that CBD elevated the level of cAMP (a known upstream regulator of TRIB3) (ref. 52 and Figure 8C), highlighting the putative role of a G_s-coupled receptor in initiating its antiinflammatory actions. We also demonstrated that sebocytes express G_s-coupled A2a receptors (which have already been shown to mediate antiinflammatory actions of CBD) (ref. 53 and Supplemental Figure 16, A–C). Further, the specific A2a antagonist (ZM) was able to prevent upregulation of TRIB3 upon CBD treatment (Figure 8D). Then, we attempted to confirm the functional presence of the putative antiinflammatory A2a receptor→cAMP→TRIB3⊣NF-κB axis. We found that coadministration of ZM abrogated the antiinflammatory action of CBD (Figure 8E). Moreover, we were also able to show that it abolished the NF-κB–inhibitory action of CBD (Figure 8F). Taken together, these data strongly argue that A2a receptor might be the primary orchestrator of the antiinflammatory actions of CBD. It should also be noted that, according to the data published by Carrier et al. (68), CBD-mediated activation of A2a receptor is very likely to be an indirect action, realized by the primary inhibition of the equilibrative nucleoside transporter(s) (e.g., ENT1, which mediates adenosine uptake of the cells) and the subsequently elevated "adenosine tone."

Collectively, our data introduce the phytocannabinoid CBD as a potent "universal" anti-acne agent, possessing a unique "triple anti-acne" profile (Figure 9). Multiple human studies have already investigated the safety of CBD (13, 14). Furthermore, it is already in use in many countries in clinical practice without any significant side effects (Sativex) (16). This is especially promising, because the currently available, most effective anti-acne agent, isotretinoin, is known to cause serious side effects (2, 69, 70). These data, together with our current findings, point to a promising, cost-effective, and, likely, well-tolerated new strategy for treating acne vulgaris, the most common human skin disease.

To the best of our knowledge, the exact pharmacokinetics of CBD in the human body is unknown, and there are no data in the literature on the (expected) intracutaneous accumulation of Sativex-derived, systemically applied CBD. However, given the extensively documented accumulation of phytocannabinoids from smoked marijuana in the pilosebaceous unit (where they become incorporated into the hair shaft) (71, 72), it is very likely that CBD can reach the sebaceous glands as well, can accumulate, and may well reach "therapeutically sufficient" concentrations there.

Moreover, it is very important to note that, besides the systemic application, one should keep in mind the possibility of the topical administration. Although the levels of CBD seen in the plasma of patients receiving Sativex are below (73) the CBD doses (= lower micromolar range) that exerted the most robust effects in our studies, such doses could easily be achieved after topical CBD application, using appropriate vehicles already used in current standard acne management. Due to its high lipophilicity, CBD is expected to preferentially enter the skin via the transfollicular route and to accumulate in the sebaceous gland (74, 75). Of great importance, such an accumulation has been documented already

for multiple topically applied lipophilic compounds, e.g., for steroid hormones (76) or photosensitizers (77), etc., arguing that the CBD doses tested here are translationally absolutely relevant.

All in all, our novel data, along with intriguing literature findings, strongly encourage the future study in clinical trials of whether either systemic or topical application of CBD and/or appropriate modulation of the related signaling pathways (Figure 9) deserves full clinical exploration as a potent, novel class of anti-acne agents.

Methods

More details regarding the methods are available in the Supplemental Methods.

Cell culturing, determination of intracellular lipids, investigation of the lipidome. Human immortalized SZ95 sebocytes (19) were cultured as described previously (12, 38). For semiquantitative detection of sebaceous lipids, Oil Red O staining was applied, whereas for quantitative measurements, fluorescent Nile Red staining was applied, as detailed in our previous work (12, 38). The sebaceous lipidome was analyzed by a HPLC-ToF/MS method as described previously (78).

Determination of viability, apoptosis, necrosis, and cellular proliferation. Viability was assessed by MTT assay (Sigma-Aldrich) as described previously (10, 12). Apoptotic and necrotic processes were investigated by combined $DilC_1(5)$ and SYTOX Green staining (Life Technologies), measuring the alterations in the mitochondrial membrane potential and in the plasma membrane permeability, respectively, as described previously (10, 12). The degree of cellular growth was determined in 96-well plate format by measuring the DNA content of the wells using the CyQUANT Cell Proliferation Assay Kit (Life Technologies), according to the manufacturer's protocol.

Q-PCR. Q-PCR was performed as detailed in our previous reports (12, 38). PCR amplification was performed by using TaqMan primers and probes (assay ID-s: Hs00174128_m1 for *TNFA*, Hs00218912_m1 for *TRPV1*, Hs00275032_m1 for *TRPV2*, Hs00222101_m1 for *TRPV4*, Hs00175798_m1 for *TRPA1*, Hs00375481_m1 for *TRPM8*, Hs00189038_m1 for cathelicidin, Hs00174097_m1 for *IL1B*, Hs00985639_m1 for *IL6*, Hs01032443_m1 for Ki67 (*MKI67*), Hs00942766_s1 for *NRIP1*, Hs01082394_m1 for *TRIB3*, Hs00261256_m1 for *ARHGAP9*, and Hs00169123_m1 for A2a receptor [*ADORA2A*]) and the TaqMan universal PCR master mix protocol (Applied Biosystems). As internal controls, transcripts of glyceraldehyde 3-phosphate dehydrogenase (*GAPDH*), peptidyl-prolyl isomerase A (cyclophilin A; *PPIA*), and 18S ribosomal RNA (*18S*) (assay IDs: Hs99999905_m1, Hs 99999904_m1, and Hs99999901_s1, respectively) were determined.

Immunocytochemistry. Expression of TRP channels and adenosine A2a receptor was investigated by using TRPV1-specific (Sigma-Aldrich); TRPV2-, TRPA1-, TRPM8-, A2a-specific (all from AbCam); and TRPV4-specific (Alomone Labs) primary antibodies (all produced in rabbit), and Alexa Fluor 488–conjugated rabbit IgG Fc segment-specific secondary antibodies (developed in goat; Life Technologies). Nuclei were visualized using DAPI (Vector Laboratories). As negative controls, the appropriate primary antibodies were omitted from the procedure.

Western blotting. Western blotting was performed as described previously (12, 38) by using rabbit anti-human P-P65, NRIP1, and TRIB3 (all from Novus Biologicals); rabbit anti-human ERK1/2 and mouse anti-human P-ERK1/2 (both from Santa Cruz); mouse anti-human P-IκBα (Cell Signaling); or the above mentioned primary antibodies.

As secondary antibodies, horseradish peroxidase–conjugated rabbit or mouse IgG Fc segment–specific antibodies (developed in goat and sheep, respectively; Bio-Rad) were used. Densitometric analysis of the signals was performed by using ImageJ software (NIH). To assess equal loading, when indicated, membranes were reprobed with anti–β-actin antibodies and visualized as described above.

Full-thickness hSOC and sample preparations. Biopsies of intact human scalp and arm skin samples were obtained from 4 women (20). Lipid production and cellular proliferation were determined by using Oil Red O staining and MKI67 labeling. Images were analyzed by ImageJ image analysis software (NIH).

RNA_i. RNAi was performed according to our optimized protocols (12, 38). SZ95 sebocytes were transfected with specific Stealth RNAi oligonucleotides (40 nM) against NRIP1 (IDs: HSS112045 ["siNRIP1a"] and HSS112046 ["siNRIP1b"]), TRIB3 (IDs: HSS184051 ["siTRIB3a"] and HSS184052 ["siTRIB3b"]), TRPV1 (IDs: HSS111306 ["siV1a"] and HSS111304 ["siV1b"]), TRPV2 (IDs: HSS122144 ["siV2a"] and HSS122145 ["siV2b"]), and TRPV4 (IDs: HSS126973 ["siV4a"] and HSS126974 ["siV4b"]) using Lipofectamine 2000 (all from Life Technologies). For controls, RNAi Negative Control Duplexes (Scrambled RNAi "medium") were applied.

Microarray analysis. Gene expression analysis of 3 independent sets of control and CBD-treated SZ95 sebocytes (10 μM CBD for 24 hours) was performed by using Human Whole Genome Oligo Microarray (44K) (Agilent Technologies). Alterations in the gene expression were regarded as significant if (a) there were at least 2-fold changes in the corresponding levels; (b) the changes were equidirectional in all cases; and (c) global, corrected *P* values were less than 0.05. Evaluation, GSEA, and Gene Ontology analysis (BiNGO) of the results were performed by Abiomics Ltd. (http://www.abiomics.eu). Data have been deposited in the NCBI Gene Expression Omnibus (79) and are accessible through GEO series accession number GSE57571 (http://www.ncbi.nlm.nih.gov/geo/query/acc.cgi?acc=GSE57571).

Determination of the intracellular cAMP concentration (ELISA). SZ95 sebocytes were treated for 1 hour with vehicle or CBD (10 μM). Cells were then lysed (cell density: 10^7 cells per ml), and lysates were assayed immediately according to the manufacturer's protocol, using Parameter Cyclic AMP Assay (R&D Systems). Evaluation of the data was performed by using the Four Parameter Logistic Curve online data analysis tool of MyAssays Ltd. (http://www.myassays.com/four-parameter-logistic-curve.assay).

Patch-clamp analysis and fluorescent Ca^{2+} imaging. Whole-cell patch-clamp recordings in the voltage-clamp configuration were performed using an Axopatch 200A amplifier (Molecular Devices) or by using an EPC-10 amplifier. Alterations in the $[Ca^{2+}]_{IC}$ were determined following 1 μM Fluo-4 AM loading by Fluorescent Image Plate Reader, as described in our previous report (80).

Statistics. Data were analyzed by IBM SPSS Statistics 19 (SPSS Inc.) software, using Student's 2-tailed 2 sample *t* test or 1-way ANOVA with Bonferroni's and Dunnett's post-hoc probes. *P* values of less than 0.05 were regarded as significant. Homogeneity of variances was analyzed by Levene's test. If Levene's test indicated inhomogeneity of variances, Games-Howel test was used instead of Bonferroni.

Study approval. This study was approved by the Institutional Research Ethics Committee of the University of Lübeck and adhered to the Declaration of Helsinki principle guidelines. Study subjects provided informed consent prior to their participation.

Acknowledgments

This research was supported by Hungarian ("Lendület" LP2011-003/2013, OTKA 101761, OTKA 105369, TÁMOP-4.2.2./A-11/1/KONV-2012-0025) and European Union (FP7-REGPOT-2008-1/229920) research grants as well as grants from the Belgian Federal Government (IUAP P7/13), the Research Foundation-Flanders (G.0825.11), the Research Council of the KU Leuven (PF-TRPLe), and the Italian Ministry of Health (RF-2010-2316435). A. Oláh was a recipient of the Richter "Talentum" Fellowship and supported by the European Union and the State of Hungary, cofinanced by the European Social Fund in the framework of TÁMOP 4.2.4. A/2-11-1-2012-0001 "National Excellence Program." B.I. Tóth was supported by the People Programme (Marie Curie Actions) of the European Union's Seventh Framework Programme (FP7/2007-2013) under REA grant agreement no. 330489.

Address correspondence to: Tamás Bíró, University of Debrecen, Nagyerdei krt. 98. Debrecen, H-4032, Hungary. Phone: 3652.255.575; E-mail: biro.tamas@med.unideb.hu.

1. Zouboulis CC, et al. What is the pathogenesis of acne? *Exp Dermatol*. 2005;14(2):143–152.
2. Kurokawa I, et al. New developments in our understanding of acne pathogenesis and treatment. *Exp Dermatol*. 2009;18(10):821–832.
3. Demuth DG, Molleman A. Cannabinoid signaling. *Life Sci*. 2006;78(6):549–563.
4. Abood ME, Sorensen RG, Stella N, eds. *endoCANNABINOIDS*. New York, New York, USA: Springer Science+Business Media New York; 2013.
5. Di Marzo V. Targeting the endocannabinoid system: to enhance or reduce? *Nat Rev Drug Discov*. 2008;7(5):438–455.
6. Russo EB. Taming THC: potential cannabis synergy and phytocannabinoid-terpenoid entourage effects. *Br J Pharmacol*. 2011;163(7):1344–1364.
7. Bíró T, et al. The endocannabinoid system of the skin in health and disease: novel perspectives and therapeutic opportunities. *Trends Pharmacol Sci*. 2009;30(8):411–420.
8. Kupczyk P, Reich A, Szepietowski JC. Cannabinoid system in the skin - a possible target for future therapies in dermatology. *Exp Dermatol*. 2009;18(8):669–679.
9. Telek A, et al. Inhibition of human hair follicle growth by endo- and exocannabinoids. *FASEB J*. 2007;21(13):3534–3541.
10. Tóth BI, et al. Endocannabinoids modulate human epidermal keratinocyte proliferation and survival via the sequential engagement of cannabinoid receptor-1 and transient receptor potential vanilloid-1. *J Invest Dermatol*. 2011;131(5):1095–1104.
11. Karsak M, et al. Attenuation of allergic contact dermatitis through the endocannabinoid system. *Science*. 2007;316(5830):1494–1497.
12. Dobrosi N, et al. Endocannabinoids enhance lipid synthesis and apoptosis of human sebocytes via cannabinoid receptor-2-mediated signaling. *FASEB J*. 2008;22(10):3685–3695.
13. Zuardi AW, et al. Cannabidiol, a Cannabis sativa constituent, as an antipsychotic drug. *Braz J Med Biol Res*. 2006;39(4):421–429.
14. Zuardi AW, et al. Cannabidiol monotherapy for treatment-resistant schizophrenia. *J Psychopharmacol*. 2006;20(5):683–686.
15. Pertwee RG. The diverse CB1 and CB2 receptor pharmacology of three plant cannabinoids: Δ9-tetrahydrocannabinol, cannabidiol and Δ9-tetrahydrocannabivarin. *Br J Pharmacol*. 2008;153(2):199–215.
16. Pertwee RG. Cannabinoid pharmacology: the first 66 years. *Br J Pharmacol*. 2006; 147(suppl 1):S163–S171.
17. NIH. Clinical Trials.gov. NIH Web site. http://clinicaltrials.gov/ct2/results?term=cannabidiol. Accessed July 8, 2013.
18. Mirshahpanah P, Maibach HI. Models in acnegenesis. *Cutan Ocul Toxicol*. 2007;26(3):195–202.
19. Zouboulis CC, Seltmann H, Neitzel H, Orfanos CE. Establishment and characterization of an immortalized human sebaceous gland cell line (SZ95). *J Invest Dermatol*. 1999;113(6):1011–1020.
20. Lu Z, Hasse S, Bodó E, Rose C, Funk W, Paus R. Towards the development of a simplified long-term organ culture method for human scalp skin and its appendages under serum-free conditions. *Exp Dermatol*. 2007;16(1):37–44.
21. Wróbel A, et al. Differentiation and apoptosis in human immortalized sebocytes. *J Invest Dermatol*. 2003;120(2):175–181.
22. Makrantonaki E, Zouboulis CC. Testosterone metabolism to 5α-dihydrotestosterone and synthesis of sebaceous lipids is regulated by the peroxisome proliferator-activated receptor ligand linoleic acid in human sebocytes. *Br J Dermatol*. 2007;156(3):428–432.
23. Rey AA, Purrio M, Viveros M-P, Lutz B. Biphasic effects of cannabinoids in anxiety responses: CB1 and GABA(B) receptors in the balance of GABAergic and glutamatergic neurotransmission. *Neuropsychopharmacology*. 2012;37(12):2624–2634.
24. Melnik BC, Schmitz G. Role of insulin, insulin-like growth factor-1, hyperglycaemic food and milk consumption in the pathogenesis of acne vulgaris. *Exp Dermatol*. 2009;18(10):833–841.
25. Zouboulis CC, Jourdan E, Picardo M. Acne is an inflammatory disease and alterations of sebum composition initiate acne lesions. *J Eur Acad Dermatol Venereol*. 2014;28(5):527–532.
26. Zouboulis CC, et al. A new concept for acne therapy: a pilot study with zileuton, an oral 5-lipoxygenase inhibitor. *Arch Dermatol*. 2003;139(5):668–670.
27. Schneider MR, Paus R. Sebocytes, multifaceted epithelial cells: lipid production and holocrine secretion. *Int J Biochem Cell Biol*. 2010;42(2):181–185.
28. Layton AM. Disorders of the sebaceous glands. In: Burns T, Breathnach S, Cox N, Griffiths C, eds. *Rook's Textbook of Dermatology*. 8th ed. Oxford, United Kingdom: Wiley-Blackwell; 2010:42.1–42.89.
29. Shirakawa M, Uramoto K, Harada FA. Treatment of acne conglobata with infliximab. *J Am Acad Dermatol*. 2006;55(2):344–346.
30. Szabó K, Kemény L. Studying the genetic predisposing factors in the pathogenesis of acne vulgaris. *Hum Immunol*. 2011;72(9):766–773.
31. Booz GW. Cannabidiol as an emergent therapeutic strategy for lessening the impact of inflammation on oxidative stress. *Free Radic Biol Med*. 2011;51(5):1054–1061.
32. Akopian AN, Ruparel NB, Jeske NA, Patwardhan A, Hargreaves KM. Role of ionotropic cannabinoid receptors in peripheral antinociception and antihyperalgesia. *Trends Pharmacol Sci*. 2008;30(2):79–84.
33. De Petrocellis L, et al. Plant-derived cannabinoids modulate the activity of transient receptor potential channels of ankyrin type-1 and melastatin type-8. *J Pharmacol Exp Ther*. 2008;325(3):1007–1015.
34. De Petrocellis L, et al. Effects of cannabinoids and cannabinoid-enriched Cannabis extracts on TRP channels and endocannabinoid metabolic enzymes. *Br J Pharmacol*. 2011;163(7):1479–1494.
35. Bisogno T, et al. Molecular targets for cannabidiol and its synthetic analogues: effect on vanilloid VR1 receptors and on the cellular uptake and enzymatic hydrolysis of anandamide. *Br J Pharmacol*. 2001;134(4):845–852.
36. Qin N, Neeper MP, Liu Y, Hutchinson TL, Lubin ML, Flores CM. TRPV2 is activated by cannabidiol and mediates CGRP release in cultured rat dorsal root ganglion neurons. *J Neurosci*. 2008;28(24):6231–6238.
37. De Petrocellis L, et al. Cannabinoid actions at TRPV channels: effects on TRPV3 and TRPV4 and their potential relevance to gastrointestinal inflammation. *Acta Physiol (Oxf)*. 2012;204(2):255–266.
38. Tóth BI, et al. Transient receptor potential vanilloid-1 signaling as a regulator of human sebocyte biology. *J Invest Dermatol*. 2009;129(2):329–339.
39. Clapham DE. Transient Receptor Potential (TRP) channels. In: Squire LR, ed. *Encyclopedia Of Neuroscience*. Vol. 9. Oxford, United Kingdom: Oxford Academic Press; 2009:1109–1133.
40. Subramanian A, et al. Gene set enrichment analysis: a knowledge-based approach for interpreting genome-wide expression profiles. *Proc Natl Acad Sci U S A*. 2005;102(43):15545–15550.
41. Mootha VK, et al. PGC-1α-responsive genes involved in oxidative phosphorylation are coordinately downregulated in human diabetes. *Nat Genet*. 2003;34(3):267–273.
42. Broad Institute. Gene Set Enrichment Analysis. http://www.broadinstitute.org/gsea/index.jsp. Broad Institute Web site. Updated January 23, 2014. Accessed June 16, 2014.

43. Melnik BC, Schmitz G. Are therapeutic effects of antiacne agents mediated by activation of FoxO1 and inhibition of mTORC1? *Exp Dermatol*. 2013;22(7):502–504.
44. The Gene Ontology Consortium. The Gene Ontology Database. The Gene Ontology Web site. homepage. http://www.geneontology.org/. Accessed June 16, 2014.
45. Gene Ontology Consortium. The Sequence Ontology Project homepage. The Sequence Ontology Web site. http://www.sequenceontology.org/. Accessed June 16, 2014.
46. Ang BK, et al. ArhGAP9, a novel MAP kinase docking protein, inhibits Erk and p38 activation through WW domain binding. *J Mol Signal*. 2007;2:1.
47. Roskoski R. ERK1/2 MAP kinases: structure, function, and regulation. *Pharmacol Res*. 2012;66(2):105–143.
48. Leonardsson G, et al. Nuclear receptor corepressor RIP140 regulates fat accumulation. *Proc Natl Acad Sci U S A*. 2004;101(22):8437–8442.
49. Lee D-Y, et al. Sebocytes express functional cathelicidin antimicrobial peptides and can act to kill Propionibacterium acnes. *J Invest Dermatol*. 2008;128(7):1863–1866.
50. Wu M, Xu LG, Zhai Z, Shu HB. SINK is a p65-interacting negative regulator of NF-κB-dependent transcription. *J Biol Chem*. 2003;278(29):27072–27079.
51. Kozela E, et al. Cannabinoids Δ9-tetrahydrocannabinol and cannabidiol differentially inhibit the lipopolysaccharide-activated NF-κB and interferon-β/STAT proinflammatory pathways in BV-2 microglial cells. *J Biol Chem*. 2010;285(3):1616–1626.
52. Zou T, et al. TRB3 mediates homocysteine-induced inhibition of endothelial cell proliferation. *J Cell Physiol*. 2011;226(11):2782–2789.
53. Ribeiro A, et al. Cannabidiol, a non-psychotropic plant-derived cannabinoid, decreases inflammation in a murine model of acute lung injury: role for the adenosine A(2A) receptor. *Eur J Pharmacol*. 2012;678(1–3):78–85.
54. Wilkinson JD, Wiliamson EM. Cannabinoids inhibit human keratinocyte proliferation through a non-CB1/CB2 mechanism and have a potential therapeutic value in the treatment of psoriasis. *J Dermatol Sci*. 2007;45(2):87–92.
55. Appendino G, et al. Antibacterial cannabinoids from Cannabis sativa: a structure-activity study. *J Nat Prod*. 2008;71(8):1427–1430.
56. Ananthapadmanabhan KP, Mukherjee S, Chandar P. Stratum corneum fatty acids: their critical role in preserving barrier integrity during cleansing. *Int J Cosmet Sci*. 2013;35(4):337–345.
57. Russo EB, Burnett A, Hall B, Parker KK. Agonistic properties of cannabidiol at 5-HT1a receptors. *Neurochem Res*. 2005;30(8):1037–1043.
58. Kathmann M, Flau K, Redmer A, Tränkle C, Schlicker E. Cannabidiol is an allosteric modulator at mu- and delta-opioid receptors. *Naunyn Schmiedebergs Arch Pharmacol*. 2006;372(5):354–361.
59. Rimmerman N, et al. Direct modulation of the outer mitochondrial membrane channel, voltage-dependent anion channel 1 (VDAC1) by cannabidiol: a novel mechanism for cannabinoid-induced cell death. *Cell Death Dis*. 2013;4:e949.
60. Ross RA. The enigmatic pharmacology of GPR55. *Trends Pharmacol Sci*. 2009;30(3):156–163.
61. Shi H, Halvorsen YD, Ellis PN, Wilkison WO, Zemel MB. Role of intracellular calcium in human adipocyte differentiation. *Physiol Genomics*. 2000;3(2):75–82.
62. Zhang LL, et al. Activation of transient receptor potential vanilloid type-1 channel prevents adipogenesis and obesity. *Circ Res*. 2007;100(7):1063–1070.
63. Takahashi Y, et al. TRB3 suppresses adipocytes differentiation by negatively regulating PPARγ transcriptional activity. *J Lipid Res*. 2008;49(4):880–892.
64. Salazar M, et al. Cannabinoid action induces autophagy-mediated cell death through stimulation of ER stress in human glioma cells. *J Clin Invest*. 2009;119(5):1359–1372.
65. Salazar M, et al. The pseudokinase tribbles homologue-3 plays a crucial role in cannabinoid anticancer action. *Biochim Biophys Acta*. 2013;1831(10):1573–1578.
66. Juknat A, et al. Microarray and pathway analysis reveal distinct mechanisms underlying cannabinoid-mediated modulation of LPS-induced activation of BV-2 microglial cells. *PLoS One*. 2013;8(4):e61462.
67. Mungrue IN, et al. CHAC1/MGC4504 is a novel proapoptotic component of the unfolded protein response, downstream of the ATF4-ATF3-CHOP cascade. *J Immunol*. 2009;182(1):466–476.
68. Carrier EJ, Auchampach JA, Hillard CJ. Inhibition of an equilibrative nucleoside transporter by cannabidiol: a mechanism of cannabinoid immunosuppression. *Proc Natl Acad Sci U S A*. 2006;103(20):7895–7900.
69. Ellis CN, Krach KJ. Uses and complications of isotretinoin therapy. *J Am Acad Dermatol*. 2001;45(5):S150–S157.
70. Rigopoulos D, Larios G, Katsambas AD. The role of isotretinoin in acne therapy: why not as first-line therapy? facts and controversies. *Clin Dermatol*. 2010;28(1):24–30.
71. Kintz P, Cirimele V, Mangin P. Testing human hair for cannabis. II. Identification of THC-COOH by GC-MS-NCI as a unique proof. *J Forensic Sci*. 1995;40(4):619–622.
72. Skopp G, Strohbeck-Kuehner P, Mann K, Hermann D. Deposition of cannabinoids in hair after long-term use of cannabis. *Forensic Sci Int*. 2007;170(1):46–50.
73. Karschner EL, Darwin WD, Goodwin RS, Wright S, Huestis MA. Plasma cannabinoid pharmacokinetics following controlled oral delta9-tetrahydrocannabinol and oromucosal cannabis extract administration. *Clin Chem*. 2011;57(1):66–75.
74. Lodzki M, et al. Cannabidiol-transdermal delivery and anti-inflammatory effect in a murine model. *J Control Release*. 2003;93(3):377–387.
75. Tubaro A, et al. Comparative topical anti-inflammatory activity of cannabinoids and cannabivarins. *Fitoterapia*. 2010;81(7):816–819.
76. Hueber F, Wepierre J, Schaefer H. Role of transepidermal and transfollicular routes in percutaneous absorption of hydrocortisone and testosterone: in vivo study in the hairless rat. *Skin Pharmacol*. 1992;5(2):99–107.
77. Togsverd-Bo K, et al. Porphyrin biodistribution in UV-exposed murine skin after methyl- and hexyl-aminolevulinate incubation. *Exp Dermatol*. 2012;21(4):260–264.
78. Camera E, et al. Comprehensive analysis of the major lipid classes in sebum by rapid resolution high-performance liquid chromatography and electrospray mass spectrometry. *J Lipid Res*. 2010;51(11):3377–3388.
79. Edgar R, Domrachev M, Lash AE. Gene Expression Omnibus: NCBI gene expression and hybridization array data repository. *Nucleic Acids Res*. 2002;30(1):207–210.
80. Borbíró I, et al. Activation of transient receptor potential vanilloid-3 inhibits human hair growth. *J Invest Dermatol*. 2011;131(8):1605–1614.